Cellular/Molecular

Tonic $GABA_A$ Conductance Favors Spike-Timing-Dependent over Theta-Burst-Induced Long-Term Potentiation in the Hippocampus

Yulia Dembitskaya,[1,2] Yu-Wei Wu,[1,3] and Alexey Semyanov[1,2,4]

[1]RIKEN Brain Science Institute, Saitama 351-0198, Japan, [2]Shemyakin-Ovchinnikov Institute of Bioorganic Chemistry, Moscow, 117997, Russia, [3]Institute of Molecular Biology, Academia Sinica, Taipei 11529, Taiwan, and [4]Sechenov First Moscow State Medical University, Moscow, 119146, Russia

Synaptic plasticity is triggered by different patterns of network activity. Here, we investigated how LTP in CA3-CA1 synapses induced by different stimulation patterns is affected by tonic $GABA_A$ conductances in rat hippocampal slices. Spike-timing-dependent LTP was induced by pairing Schaffer collateral stimulation with antidromic stimulation of CA1 pyramidal neurons. Theta-burst-induced LTP was induced by theta-burst stimulation of Schaffer collaterals. We mimicked increased tonic $GABA_A$ conductance by bath application of 30 μM GABA. Surprisingly, tonic $GABA_A$ conductance selectively suppressed theta-burst-induced LTP but not spike-timing-dependent LTP. We combined whole-cell patch-clamp electrophysiology, two-photon Ca^{2+} imaging, glutamate uncaging, and mathematical modeling to dissect the mechanisms underlying these differential effects of tonic $GABA_A$ conductance. We found that Ca^{2+} transients during pairing of an action potential with an EPSP were less sensitive to tonic $GABA_A$ conductance-induced shunting inhibition than Ca^{2+} transients induced by EPSP burst. Our results may explain how different forms of memory are affected by increasing tonic $GABA_A$ conductances under physiological or pathologic conditions, as well as under the influence of substances that target extrasynaptic $GABA_A$ receptors (e.g., neurosteroids, sedatives, antiepileptic drugs, and alcohol).

Key words: **extrasynaptic signaling; $GABA_A$ receptor; synaptic plasticity; tonic inhibition**

Significance Statement

Brain activity is associated with neuronal firing and synaptic signaling among neurons. Synaptic plasticity represents a mechanism for learning and memory. However, some neurotransmitters that escape the synaptic cleft or are released by astrocytes can target extrasynaptic receptors. Extrasynaptic $GABA_A$ receptors mediate tonic conductances that reduce the excitability of neurons by shunting. This results in the decreased ability for neurons to fire action potentials, but when action potentials are successfully triggered, tonic conductances are unable to reduce them significantly. As such, tonic $GABA_A$ conductances have minimal effects on spike-timing-dependent synaptic plasticity while strongly attenuating the plasticity evoked by EPSP bursts. Our findings shed light on how changes in tonic conductances can selectively affect different forms of learning and memory.

Introduction

Tonic conductances mediated by $GABA_A$ receptors have received significant attention over the last two decades (Brickley et al., 1996; Semyanov et al., 2004; Farrant and Nusser, 2005; Glykys and Mody, 2007a; Brickley and Mody, 2012). Often referred to as tonic current or tonic inhibition, this is thought to be a mechanism that decreases the excitability of specific cell populations in the brain (Semyanov, 2003; Semyanov et al., 2003; Ade et al., 2008; Vardya et al., 2008; Urban-Ciecko et al., 2010). The tonic $GABA_A$ conductance is set by concentrations of ambient GABA, the expression of high-affinity $GABA_A$ receptors, and the presence of endogenous and exogenous modulators of these receptors (Semyanov et al., 2003; Stell et al., 2003; Scimemi et al., 2005; Glykys and Mody, 2007b; Song et al., 2013). Endogenous modulators include neurosteroids, the concentrations of which change in the brain during puberty, pregnancy, and the ovarian cycle (Herd et al., 2007; Maguire and Mody, 2007, 2008). The corresponding changes in the tonic $GABA_A$ conductance can promote stress, anxiety, and depression (Maguire and Mody, 2007, 2008; Shen et al., 2007; MacKenzie and Maguire,

Received Sep. 2, 2019; revised Mar. 21, 2020; accepted Apr. 15, 2020.

Author contributions: Y.D., Y.-W.W., and A.S. designed research; Y.D. and Y.-W.W. performed research; Y.D. and Y.-W.W. analyzed data; A.S. wrote the first draft of the paper; A.S. edited the paper; A.S. wrote the paper.

This work was supported by Russian Foundation for Basic Research Grant 17-00-00409 to A.S. We thank Dr. Tanja Brenner for performing preliminary experiments.

The authors declare no competing financial interests.

Correspondence should be addressed to Alexey Semyanov at alexeysemyanov@gmail.com.

https://doi.org/10.1523/JNEUROSCI.2118-19.2020

2013). A socially relevant exogenous factor that augments the tonic $GABA_A$ conductance is ethanol (Wei et al., 2004; Hanchar et al., 2005). Hence, acute ethanol intake impairs synaptic plasticity, learning, and memory (McCool, 2011). In contrast, chronic ethanol abuse downregulates the GABAergic system (Davies, 2003).

Indeed, the tonic $GABA_A$ conductance is involved in far more complex neuronal computations than would be expected for a simple inhibitory action. Tonic conductances modulate neuronal gain during synaptic excitation in small-size cells (e.g., cerebellar granule cells) and neuronal offset in larger cells (e.g., hippocampal pyramidal neurons) (Mitchell and Silver, 2003; Semyanov et al., 2004; Pavlov et al., 2009). The tonic $GABA_A$-conductance mediated decrease in cellular input resistance reduces both the membrane time constant and the membrane length constant (Rall, 1969; Jack and Redman, 1971). These constants influence the shape of EPSPs, their integration, and EPSP-spike coupling in hippocampal interneurons and pyramidal cells (Wlodarczyk et al., 2013; Pavlov et al., 2014). In addition, the tonic $GABA_A$ conductance modulates synaptic plasticity and brain rhythms (Mann and Mody, 2010; Shen et al., 2010; Pavlov et al., 2014).

Moreover, the tonic activation of $GABA_A$ receptors is not always inhibitory. Immature neurons have depolarizing reversal potentials for GABA (E_{GABA}), which become hyperpolarizing in the adult brain (Ben-Ari, 2002). Nevertheless, several types of mature neurons maintain depolarizing E_{GABA}: for example, striatal projection neurons (Bracci and Panzeri, 2006), hippocampal granule cells (Chiang et al., 2012), suprachiasmatic nucleus neurons (Choi et al., 2008), vasopressin-secreting hypothalamic neurons (Haam et al., 2012), and interneurons of the hippocampus and amygdala (Banke and McBain, 2006; Woodruff et al., 2006). Low levels of tonic $GABA_A$ conductance excite hippocampal interneurons by exerting small depolarizations that recruit voltage-dependent membrane conductances (Song et al., 2011). A high level of tonic $GABA_A$ conductance inhibits these neurons by a shunting effect. The tonic activation of presynaptic $GABA_A$ receptors depolarizes hippocampal mossy fiber boutons and increases synaptic release probability (Ruiz et al., 2010).

Thus, tonic $GABA_A$ conductances influence cell excitability and the integration of synaptic inputs depending on cell size, E_{GABA}, and the magnitude of this conductance. Acute increases in tonic conductance inhibit the LTP induced by high-frequency stimulation in the hippocampus (Whissell et al., 2013). However, until now, it has remained unclear whether tonic $GABA_A$ conductances differentially affect synaptic plasticity which triggered by different neuronal network dynamics. To address this issue, we compared the effect of tonic $GABA_A$ conductances on spike-timing-dependent LTP (stLTP) induced by pairing synaptic input activation and postsynaptic cell spiking and theta-burst-induced LTP (tbLTP) induced by theta-bursts of presynaptic cell firing.

Materials and Methods

Hippocampal slice preparation

Transverse hippocampal slices were prepared from 3- to 5-week-old Sprague Dawley male rats in accordance with RIKEN regulations. Animals were anesthetized with 2-bromo-2-chloro-1,1,1-trifluoroethane (halothane) and decapitated. The brain was exposed and cooled with an ice-cold solution containing the following (in mM): 75 sucrose, 87 NaCl, 2.5 KCl, 0.5 $CaCl_2$, 1.25 NaH_2PO_4, 7 $MgCl_2$, 25 $NaHCO_3$, 1 Na-ascorbate, and 25 D-glucose. Hippocampi from both hemispheres were isolated and placed in an agar block. Transverse slices (350-400 μm) were prepared with a vibrating microtome (Microm HM 650V, Thermo Fisher Scientific) and left to recover for 20 min at 34°C and then for 40 min in an interface chamber with storage solution containing the following (in mM): 127 NaCl, 2.5 KCl, 1.25 NaH_2PO_4, 2 $MgCl_2$, 1 $CaCl_2$, 25 $NaHCO_3$, and 11 D-glucose. The slices were then transferred to the recording chamber and continuously perfused with a recording solution containing the following (in mM): 127 NaCl, 2.5 KCl, 1.25 NaH_2PO_4, 1 $MgCl_2$, 2 $CaCl_2$, 25 $NaHCO_3$, and 11 D-glucose at 34°C. All solutions were saturated with 95% O_2 and 5% CO_2. Osmolarity was adjusted to 295 ± 5 mOsm; 5 μM 3-[[(3,4-dichlorophenyl)methyl]amino]propyl] diethoxymethyl) phosphonic acid (CGP52432) and 400 μM (S)-α-methyl-4-carboxyphenylglycine (S-MCPG) were routinely added to the solution to block $GABA_B$ and metabotropic glutamate receptors, respectively. Cells were visually identified under infrared DIC using an Olympus BX-61 microscope (Olympus).

Electrophysiology

A glass electrode, with a resistance of 3-5 MΩ, filled with the extracellular solution, was placed in *stratum radiatum* for field potential recordings (see Fig. 1*a*). Synaptic responses were evoked by stimulation via two bipolar stainless-steel electrodes (FHC). Theta-burst stimulation of Schaffer collaterals (SCs) was performed with the electrode placed in the *stratum radiatum* >200 μm from the recording site to induce tbLTP. Theta-burst stimulation consisted of 10 bursts with a 200 ms interburst interval; each burst consisted of 4 pulses with a duration of 0.2 ms at a frequency of 100 Hz. stLTP was induced with one electrode placed in the *stratum radiatum* to trigger glutamate release from SC, and another electrode placed in the *stratum oriens* to trigger antidromic (AD) action potentials (APs) in postsynaptic CA1 pyramidal neurons (AD stimulation). SC stimulation was followed by a 10 ms pause before AD stimulation, and this paired stimulation was repeated every 6 seconds for 10 min. Stimulus strength was adjusted to 30%-50% of the maximal amplitude of fEPSPs.

Whole-cell recordings in CA1 pyramidal neurons were obtained using patch electrodes with a resistance of 3-5 MΩ, filled with a solution containing the following (in mM): 130 KCH_3SO_3, 8 NaCl, 10 HEPES, 10 Na_2-phosphocreatine, 4 Na_2ATP, 0.4 NaGTP, 3 L-ascorbic acid, pH adjusted to 7.2 with KOH (osmolarity to 290 mOsm). The recording solution also contained the morphologic tracer AlexaFluor-594 (50 μM, red channel, R) and the Ca^{2+}-sensitive dye Fluo-4F (250 μM, green channel, G) for stLTP, and Fluo-5F (300 μM, green channel, G) for tbLTP. Baseline Ca^{2+} transients were significantly different for the two types of stimulation; thus, different dyes were selected to ensure that the response was within the dynamic range of each dye.

APs were induced by somatic current injections (2 ms, 1-2 nA). The membrane potential was kept at −70 mV for all recordings to ensure experimental conditions were consistent. The threshold of APs was calculated from phase portraits as the membrane potential (V_m) when $\Delta V_m/\Delta t$ was 20 mV/ms. Input resistance was calculated from the voltage response to 500 ms current injection in a stepwise fashion from −50 to 50 pA in 10 pA steps (the I–V curves). The series resistance was typically < 20 MΩ, and data were discarded if this changed by >20% during the recording. The series resistance was compensated for by the "bridge balance" function in current-clamp mode.

Recordings were amplified with a patch-clamp amplifier, Multiclamp 700B (Molecular Devices), and digitized at 10 kHz with a NI PCI-6221 card (National Instrument). The data were visualized and stored with WinWCP software (supplied free of charge to academic users by John Dempster, University of Strathclyde).

Two-photon imaging

Cells were filled with dye for at least 20 min before imaging to ensure dye equilibration. Two-photon Ca^{2+} imaging was performed with a two-scanner FV1000-MPE laser-scanning microscope (Olympus) equipped with a mode-locked (<140 fs pulse width) tunable 720-930 nm laser Chameleon XR (Coherent). Both dyes were excited at a wavelength of 830 nm, and their fluorescence was chromatically separated and detected with two independent photomultipliers. We used the bright AlexaFluor-594 emission to identify oblique apical dendrites (~150 mm

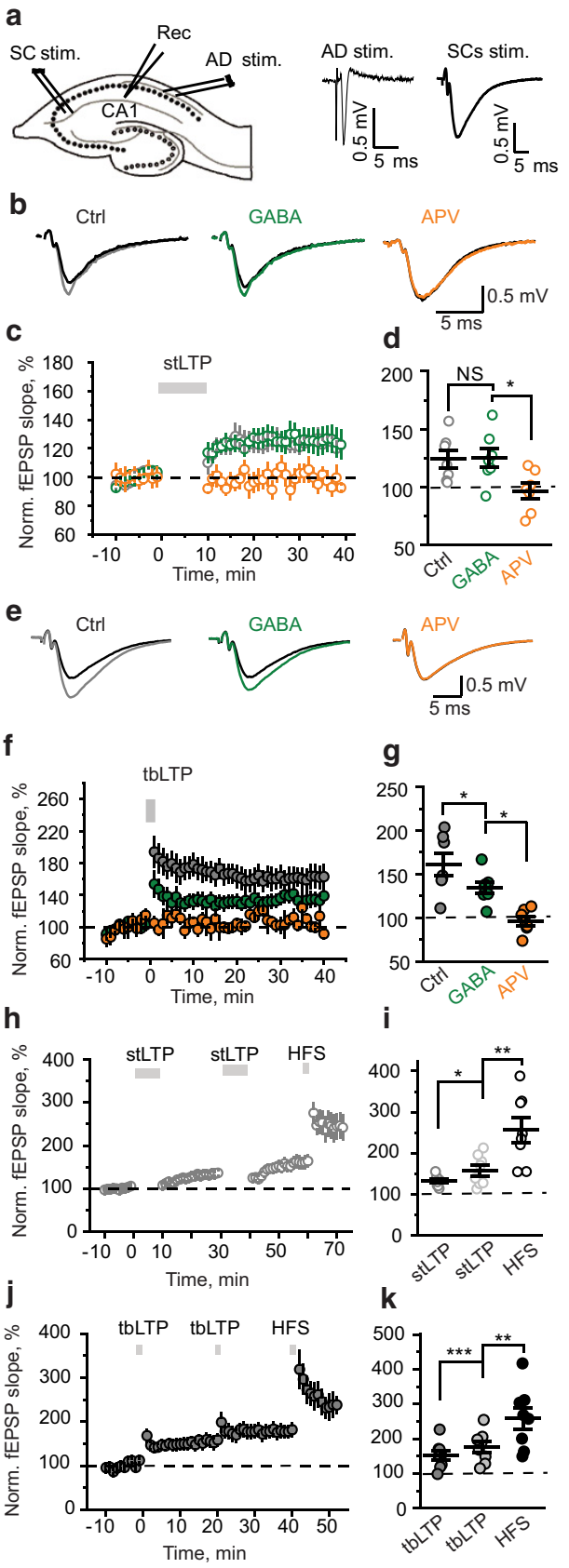

Figure 1. Tonic $GABA_A$ conductances have no effect on stLTP but suppress tbLTP. ***a***, Left, A schematic of a hippocampal slice showing the location of stimulating and recording electrodes. The recording electrode was placed in CA1 *stratum radiatum* (Rec), the first stimulating electrode on Shaffer collaterals (SC stim.), the second electrode in *stratum oriens* for AD stimulation (AD stim.). Right, AD stimulation induced an antidromic population spike, whereas SC stimulation induced fEPSP. stLTP was induced by the pairing of CS and AD stimulations; tbLTP was induced by bursts of SC stimulation. ***b***, Average fEPSPs 30-40 min after stLTP induction in control (gray), in the presence of GABA (green), and in the presence of APV (orange). Black represents fEPSPs before stLTP induction. ***c***, The time course of averaged and normalized fEPSP slope in control (gray), in the presence of GABA (green), and in the presence of APV (orange). The zero time point is the beginning of the stLTP induction protocol (gray bar). ***d***, The summary of data showing the average magnitude of stLTP 30-40 min after induction. Gray represents control (Ctrl). Green represents GABA. Orange represents APV. ***e***, Average fEPSPs 30-40 min after tbLTP induction in control (gray), in the presence of GABA (green), and in the presence of APV (orange). Black represents fEPSPs before tbLTP induction. ***f***, The time course of averaged and normalized fEPSP slope in control (gray), in the presence of GABA (green), and in the presence of APV (orange). The zero time point is the beginning of the tbLTP induction protocol (gray bar). ***g***, The summary of data showing the average magnitude of tbLTP 30-40 min after induction. Gray represents control (Ctrl). Green represents GABA. Orange represents APV. ***h***, The time course of averaged and normalized fEPSP slope showing the effect of two sequential stLTP protocols followed by HFS. ***i***, The summary of data showing the average magnitude of stLTPs and HFS-induced LTP 5-10 min after induction. ***j***, The time course of averaged and normalized fEPSP slope showing the effect of two sequential tbLTP protocols followed by HFS. ***k***, The summary of data showing the average magnitude of tbLTPs and HFS-induced LTP 5-10 min after induction. Data are mean ± SEM. NS, Not significant ($p > 0.05$). *$p < 0.05$; **$p < 0.01$; ***$p < 0.001$; two-sample *t*-test.

from the soma) and their spines. Line-scan imaging was performed to record Ca^{2+} signals in the dendritic shaft and from one to three spines. Imaging was synchronized with electrophysiological recordings. At the end of each recording, we tested that the Ca^{2+} transients were below the dye saturation level by prolonged somatic depolarization, causing cell firing and Ca^{2+} buildup in neurons. The changes in baseline Ca^{2+} levels were monitored as the ratio between baseline Fluo-4 or Fluo-5F and AlexaFluor-594 fluorescence ($G_{baseline}/R_{baseline}$). If this ratio increased during the experiment by >20%, the recordings were discarded. The dark noise of the photomultipliers was collected during each recording when the laser shutter was closed.

Glutamate uncaging

Glutamate concentration in the synaptic cleft can reach ~1 mM and decays with a time constant of 1.2 ms (Clements et al., 1992). Glutamate uncaging cannot precisely mimic this concentration profile. First, it is impossible to uncage glutamate only in the synaptic cleft without activating extrasynaptic NMDA receptors (NMDARs). Second, to obtain 1 mM of glutamate, 5–10 mM of the caged compound should be added to the bath or locally applied. This can potentially cause osmotic stress. Here we used a bath application of 400 μM 4-methoxy-7-nitroindolinyl-caged-L-glutamate, which did not produce significant osmolarity changes. Then we adjusted the duration and intensity of laser stimulation to mimic synaptically induced EPSPs of 2–3 mV [uncaging induced (u) EPSP]. Single-photon uncaging was conducted using 5–10 ms laser pulses (405 nm diode laser; FV5-LD405; Olympus) with the "point scan" mode in Fluoview software (Olympus). Uncaging spots were typically positioned at the edge of the spine heads of imaged dendrites. The Ca^{2+} transients were measured in response to (1) a single backpropagating AP (bAP) induced by somatic current injection; (2) bAP/uEPSP pairing in which a single bAP was followed by uncaging at a single dendritic spine with a 20 ms delay (the strength of uncaging was adjusted to trigger 2-3 mV uEPSP); and (3) a uEPSP burst in which uncaging was simultaneously performed at four dendritic spines 4 times at 100 Hz (the strength of uncaging was adjusted to trigger two APs).

Drugs and chemicals

All drugs were kept frozen at −20°C in 100-200 μl 1000× concentration aliquots (stock solutions). CGP52432, S-MCPG, GABA, D-APV, picrotoxin, and 4-methoxy-7-nitroindolinyl-caged L-glutamate were purchased from Tocris Cookson. AlexaFluor-594, Fluo-4F, and Fluo-5F were obtained from Invitrogen.

Data analysis

Electrophysiological data were analyzed with WinWCP and Clampfit (Molecular Devices). Imaging data were analyzed using FluoView (Olympus), ImageJ (a public domain Java image processing program by Wayne Rasband), and custom software written in LabView (National Instruments). Statistical analysis was performed using Excel (Microsoft) and Origin 8 (OriginLab). Ca^{2+} transients were represented as ΔG/R: $(G_{peak} - G_{baseline})/(R_{baseline} - R_{dark\ noise})$; the baseline Ca^{2+} level was estimated as G/R: $(G_{baseline} - G_{dark\ noise})/(R_{baseline} - R_{dark\ noise})$, where G is the Fluo-4F/Fluo-5F fluorescence and R is AlexaFluor-594 fluorescence. $G_{baseline}$ and $R_{baseline}$ are the average fluorescence levels 50-100 ms before stimulation. G_{peak} is the mean fluorescence 30-40 ms following stimulation. $G_{dark\ noise}$ and $R_{dark\ noise}$ are the dark currents of the corresponding photomultipliers. For illustration purposes, single traces were processed by a 5 point moving average, and then four or five sequential traces were averaged. The statistical significance was tested using a paired-sample, two-sample, or one-sample *t*-test when appropriate. Data are presented as mean ± SEM; and *n* indicates the number of recordings.

Mathematical modeling

Simulations were performed in the NEURON 7.1 simulation environment (Hines and Carnevale, 1997). A biophysically detailed CA1 hippocampal pyramidal cell model was modified from Poirazi et al. (2003). The implemented membrane mechanisms included location-dependent R_m (membrane resistance) and R_a (axial resistance). The model incorporated sodium, delay rectifier-, A-type, M-type, Ca^{2+}-activated potassium, and *h*-type conductances, as well as L-, R-, and T-type voltage-dependent Ca^{2+} channels (Poirazi et al., 2003). The detailed conductance densities and their subcellular distribution properties are provided in the supplementary information of Poirazi et al. (2003). The excitatory synaptic conductance was composed of AMPA receptors (AMPARs) and NMDARs (gAMPA and gNMDA): gAMPA was represented by a double exponential function with τ_{rise} of 1 ms τ_{decay} of 12 ms (Otmakhova et al., 2002); gNMDA was implemented as in Kampa et al. (2004). Six excitatory synapses were placed at six different apical oblique dendrites (apical dendrite 5, 8, 10, 18, 113, and 118) within the *stratum radiatum*. gAMPA and gNMDA were set to generate 10 pA somatic excitatory postsynaptic currents with a physiological NMDA/AMPA charge ratio in each excitatory synapse (Otmakhova et al., 2002). The tonic $GABA_A$ conductance (gGABA) with an outward-rectifying property was adapted from Pavlov et al. (2009). gGABA density was distributed homogeneously along the cell membrane and was set so as to increase the membrane conductance by 25% (1.7 mS/cm^2) with $E_{GABA} = -75$ mV to mimic experimental conditions. The initial resting membrane potential of simulated neurons was set to −70 mV, and the simulation temperature was 34°C.

Membrane potential and intracellular Ca^{2+} concentrations were simulated during bAP/EPSP pairing, and EPSP burst. For bAP/EPSP pairing, activation of six excitatory synapses was followed by somatic current injection (1.7 nA, 2 ms) to trigger a single AP with a 20 ms delay; for the EPSP burst, six excitatory synapses were activated 4 times at 100 Hz; to mimic D-APV and picrotoxin applications, gNMDA and gGABA were set to zero, respectively.

Results

Tonic $GABA_A$ conductance has no effect on stLTP but suppresses tbLTP

We recorded fEPSPs from the CA1 *stratum radiatum* of rat hippocampal slices in response to extracellular stimulation of SCs (Fig. 1*a*). Two experimental protocols were used to trigger LTP in CA3-CA1 synapses: the stLTP protocol (paired synaptic and AD stimulation repeated 100 times within 10 min) and tbLTP protocol (four synaptic stimulations at 100 Hz repeated 10 times with a 200 ms interval). Each type of LTP was entirely blocked by 50 μM D-APV (APV), an NMDAR antagonist (Fig. 1*b–g*). An increase in tonic $GABA_A$ conductance was simulated by the bath application of 30 μM GABA. Because of efficient uptake, we assumed the acting concentration of GABA to be in the low micromolar range expected under physiological conditions *in vivo*. Nevertheless, because GABAergic synapses are located on the dendritic shaft, they have fewer astrocyte processes in their vicinity and are relatively exposed to ambient GABA (Gavrilov et al., 2018). Thus, the bath application of GABA can recruit both extrasynaptic and synaptic $GABA_A$ receptors.

Table 1. Tonic $GABA_A$ conductances do not affect AP properties in the soma of CA1 pyramidal neurons[a]

	Control	GABA	Paired-sample *t*-test (*p*)
AP amplitude	107.8 ± 5.6 mV	108.7 ± 6.7 mV	0.50
AP half-width	1.47 ± 0.15 ms	1.49 ± 0.15 ms	0.19
AP threshold	−54.1 ± 4.0 mV	−54.6 ± 4.3 mV	0.45

[a]Data are mean ± SEM; $n = 7$.

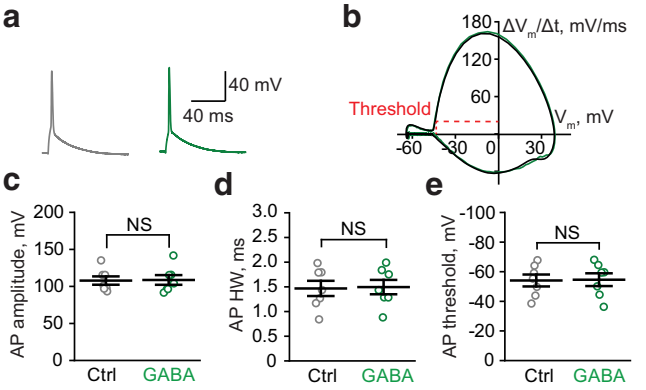

Figure 2. Tonic $GABA_A$ conductances do not affect the properties of APs. ***a***, Sample APs in control (Ctrl, gray) and in the presence of GABA (green). ***b***, Phase plots of APs do not differ in control (gray) and in the presence of GABA (green). The threshold of APs was calculated as the membrane potential (V_m) at AP velocity $\Delta V_m/\Delta t = 20$ mV/ms. The plot was low-pass filtered at the values of V_m below the AP threshold for clarity. ***c–e***, The summary of data are shown for the amplitude (***c***), half-width (HW, ***d***), and threshold (***e***) of APs in control (gray) and in the presence of GABA (green). Data are mean ± SEM. NS, Not significant ($p > 0.05$, paired-sample *t*-test).

GABA increased the membrane conductance of CA1 pyramidal neurons to 122 ± 6% of baseline ($n = 5$, $p = 0.02$, one-sample *t*-test) but did not significantly affect stLTP (fEPSP slope: 121 ± 6% of baseline in control, 30 min after stLTP induction, $n = 8$; 125 ± 9% of baseline in the presence of GABA, $n = 7$, $p = 0.753$, two-sample *t*-test; Fig. 1*b–d*). However, it reduced tbLTP by approximately half (fEPSP slope: 161 ± 13% of baseline in control, 30 min after tbLTP, $n = 7$; 130 ± 7% of baseline in the presence of GABA, $n = 8$, $p = 0.041$, two-sample *t*-test; Fig. 1*e–g*). These results suggest that, although both types of LTP are NMDAR-dependent, they are differentially affected by tonic $GABA_A$ conductances.

An alternative explanation to the differential effect of tonic $GABA_A$ conductances on two types of LTP is that stLTP is saturated with the induction protocol, which we used. When LTP is saturated, it may become insensitive to any kind of modulation. To test this possibility, we repeated the stLTP protocol twice and then applied high-frequency stimulation (HFS, 100 Hz for 1 s). The second stLTP protocol increased the magnitude of LTP, which was further increased by HFS (fEPSP slope: 132 ± 5% of baseline after first stLTP protocol, 158 ± 13% after second stLTP protocol, $p = 0.03$ for difference; 256 ± 30% after HFS, $p = 0.0012$ for the difference with second stLTP, $n = 8$, paired-sample *t*-test; Fig. 1*h,i*). Then we performed a similar experiment for tbLTP.

The second tbLTP protocol also increased the magnitude of LTP. Subsequent HFS produced an increase in LTP similar to HFS in the stLTP experiment (fEPSP slope: 152 ± 13% of baseline after first tbLTP protocol, 176 ± 16% after second tbLTP protocol, $p = 0.0003$ for difference; 258 ± 31% after HFS, $p = 0.002$ for the difference with second stLTP, $n = 8$, paired-sample t-test; Fig. 1*j*,*k*). These results indicate that neither stLTP nor tbLTP was saturated. A similar magnitude of LTP induced by HFS suggests that slices were in similar conditions in both experiments.

Tonic $GABA_A$ conductance does not affect amplitude and kinetics of somatic AP

To understand the mechanism underlying the differential effects of tonic $GABA_A$ conductances on LTP, we first tested whether tonic $GABA_A$ conductance directly modulates somatic AP amplitude and kinetics. Previous reports have suggested that the activation of extrasynaptic $GABA_A$ receptors can influence the AP waveform (Szemes et al., 2013; Xia et al., 2014). Because stLTP depends on voltage-dependent removal of the Mg^{2+}-block of NMDARs by bAP, changes in its waveform might lead to changes in the effectiveness of stLTP induction. However, we did not observe a significant change in amplitude, half-width, or threshold of somatic APs in CA1 pyramidal neurons following GABA application (Table 1; Fig. 2). This result is consistent with our finding that stLTD was not affected by tonic $GABA_A$ conductance. Indeed, APs are regenerative events, and their amplitude depends on the activation of Na^+ and K^+ conductances, which are considerably larger than the tonic $GABA_A$ conductance (Hausser et al., 2001).

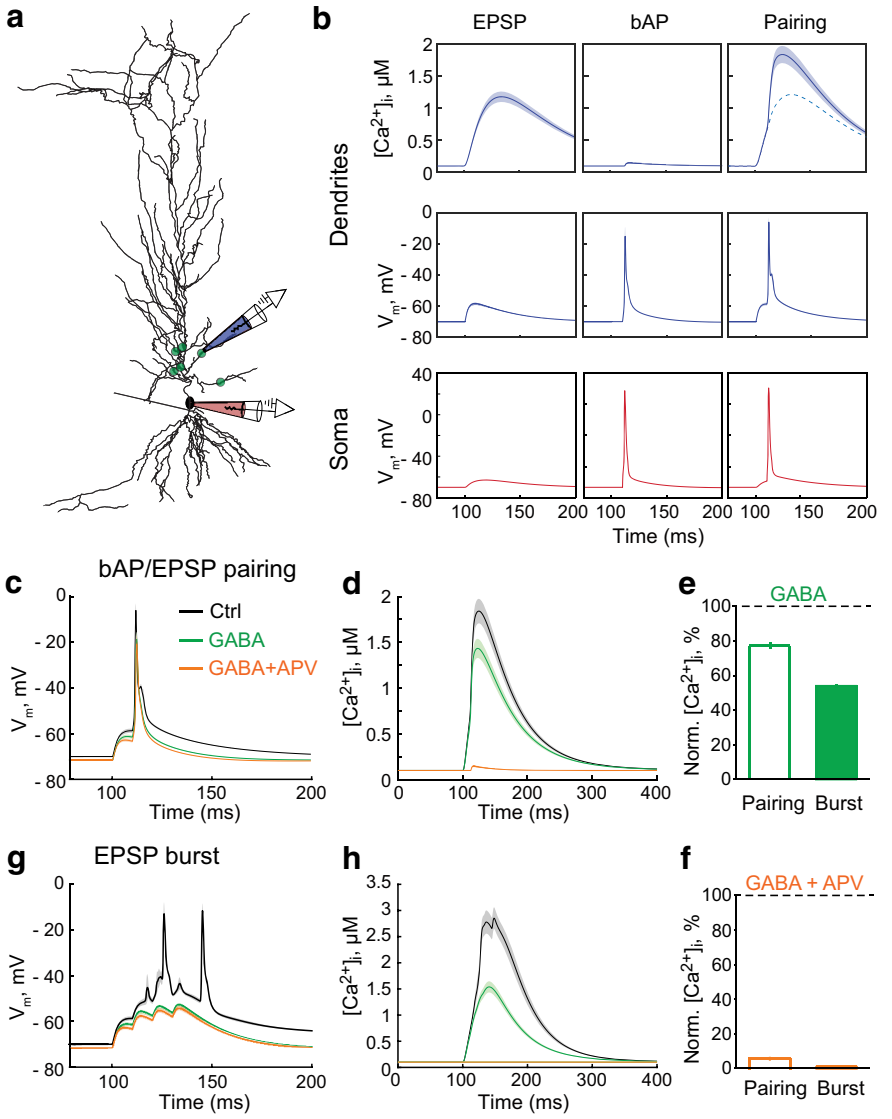

Figure 3. Tonic $GABA_A$ conductances differentially affect responses to bAP/EPSP pairing and EPSP burst in the model pyramidal neuron. ***a***, The synapse location (green dots) on the simulated pyramidal neuron. Two electrodes indicate where V_m was obtained: red, on soma; blue, on a second-order dendritic branch. The somatic electrode also indicates where the current injection used to elicit bAP occurred. ***b***, The Ca^{2+} transients in the dendrite (top row); V_m in the dendrite (middle row) and the soma (bottom row). Left column, EPSP. Middle column, bAP. Right column, bAP/EPSP pairing. $[Ca^{2+}]_i$, Intracellular Ca^{2+} concentration. ***c***, The ΔV_m to bAP/EPSP pairing in control (Ctrl, gray), on an increase in the tonic $GABA_A$ conductance (GABA, green), and subsequent blockade of NMDARs (GABA + APV, orange). ***d***, The Ca^{2+} transient in response to bAP/EPSP pairing in control (gray), and on an increase in the tonic $GABA_A$ conductance (green), and subsequent blockade of NMDARs (orange). ***e***, The summary of data on the effect of tonic $GABA_A$ conductances (GABA) on the amplitude of the Ca^{2+} transient induced by bAP/EPSP pairing (empty bar) and EPSP burst (filled bar). ***f***, The summary of data on the effect of subsequent NMDAR blockade (GABA + APV) on the amplitude of the Ca^{2+} transient induced by bAP/EPSP pairing (empty bar) and EPSP burst (filled bar). ***g***, The ΔV_m to EPSP burst in control (gray), and on an increase in the tonic $GABA_A$ conductance (green), and subsequent blockade of NMDARs (orange). ***h***, The Ca^{2+} transient in response to EPSP burst in control (gray), and on an increase in the tonic $GABA_A$ conductance (green), and subsequent blockade of NMDARs (orange).

Tonic $GABA_A$ conductance differentially affects responses to bAP/EPSP pairing and EPSP burst in model pyramidal neurons

The properties of somatic APs are determined by the high density of Na^+ and K^+ channels in the nearby triggering zone. When the AP propagates along a dendrite, the density of voltage-dependent conductances decreases; and as such, bAPs can be influenced by tonic $GABA_A$-mediated shunting as nonregenerative events (Golding et al., 2001; Groen et al., 2014; Brunner and Szabadics, 2016; but see Bereshpolova et al., 2007). To address the effects of tonic $GABA_A$ conductances on bAPs in dendritic spines and thin dendrites, we used a previously suggested mathematical model (Poirazi et al., 2003). Six synapses were simulated at proximal regions of apical oblique dendrites to induce a single multisynaptic EPSP (Fig. 3*a*). A somatic current injection (1.7 nA, 2 ms) was simulated to trigger a bAP. The pairing of an EPSP with a bAP was used to mimic a single stimulation in the stLTP protocol. The somatic AP was triggered with a 10 ms delay, matching the bAP's arrival with the peak of the EPSP. The bAP alone induced much smaller Ca^{2+} transients than the EPSP (Fig. 3*b*). The pairing of a bAP with an EPSP induced a supralinear increase in the magnitude of the Ca^{2+} transient (Nevian and Sakmann, 2004). Tonic $GABA_A$ conductance (1.7 mS/cm^2) decreased the area under the curve

Table 2. Tonic $GABA_A$ conductances reduce the ΔV_m and Ca^{2+} transient induced by EPSP burst to a greater extent than those induced by bAP/EPSP pairing in the model neuron[a]

	GABA	APV	GABA + APV
bAP/EPSP pairing			
Dendrite ΔV_m AUC	73.3 ± 0.4% (6)	87.5 ± 1.2% (6)	73.3 ± 0.7% (6)
Peak $\Delta[Ca^{2+}]_i$	76.7 ± 1.8% (6)	6.8 ± 0.7% (6)	5.6 ± 0.5% (6)
EPSP burst			
Dendrite ΔV_m AUC	48.8 ± 1.1% (6)	66.2 ± 0.2% (6)	44.6 ± 0.9% (6)
Peak $\Delta[Ca^{2+}]_i$	53.8 ± 0.9% (6)	7.6 ± 0.6% (6)	0.0 ± 0.0% (6)

[a]Data are mean ± SEM (*n*). The responses were normalized to control. GABA, the introduction of the tonic $GABA_A$ conductance; APV, removal of NMDAR conductance; GABA + APV, both.

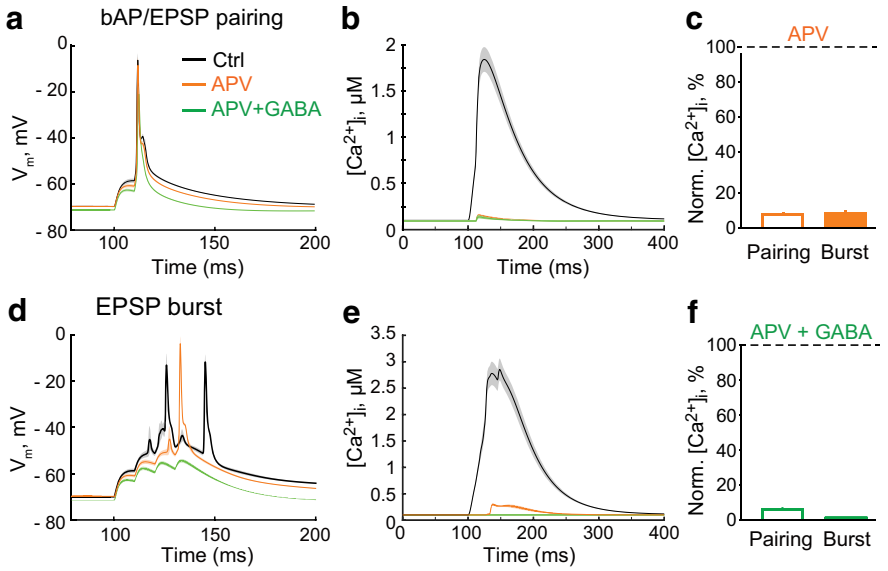

Figure 4. Effects of GABA on NMDAR-independent Ca^{2+} transients in the model neuron. ***a***, The change in V_m in response to bAP/EPSP pairing in control (Ctrl, black), and on the blockade of NMDARs (APV, orange) and subsequent increase of the tonic $GABA_A$ conductance (GABA + APV, green). ***b***, The Ca^{2+} transient in response to bAP/EPSP pairing in control (black), and on the blockade of NMDARs (orange) and subsequent increase of the tonic $GABA_A$ conductance (green). ***c***, The summary of data on the effect of the NMDAR blockade (APV, orange) and subsequent increase in the tonic $GABA_A$ conductance (GABA + APV, green) on the amplitude of the Ca^{2+} transient induced by bAP/EPSP pairing. ***d***, The summary of data on the effect of the NMDAR blockade (APV, orange) and subsequent increase in the tonic $GABA_A$ conductance (GABA + APV, green) on the amplitude of the Ca^{2+} transient induced by EPSP burst. ***e***, The change in V_m in response to EPSPs burst in control (Ctrl, black), and on blockade of NMDARs (APV, orange) and subsequent increase in the tonic $GABA_A$ conductance (GABA + APV, green). ***f***, The Ca^{2+} transient in response to EPSP burst in control (black), and on blockade of NMDARs (orange) and subsequent increase of the tonic $GABA_A$ conductance (green).

(AUC) of the ΔV_m induced by the bAP/EPSP pairing by approximately one-fourth (Table 2; Fig. 3*c*); and consequently, the amplitude of the Ca^{2+} transient was reduced by a similar degree (Table 2; Fig. 3*d*,*e*). The subsequent blockade of NMDARs nearly abolished the remaining Ca^{2+} transient (Table 2, GABA + APV; Fig. 3*d*,*f*). Notably, after introducing the tonic $GABA_A$ conductance, the blockade of NMDARs had no further effect on the AUC of ΔV_m induced by the bAP/EPSP pairing (Table 2; Fig. 3*c*). However, the blockade of NMDARs without a tonic $GABA_A$ conductance reduced the AUC of ΔV_m (Table 2; Fig. 4*a*). This NMDAR blockade also suppressed the Ca^{2+} transient produced by the bAP/EPSP pairing (Table 2; Fig. 4*b*,*c*). Thus, most Ca^{2+} entering the spine during bAP/EPSP pairing is mediated by NMDARs. Approximately one-fourth of this Ca^{2+} transient and ΔV_m was blocked by a tonic $GABA_A$ conductance.

Next, we simulated an EPSP burst similar to that in the tbLTP protocol: four EPSPs at 100 Hz were simulated at the same six synapses. The resulting EPSP burst triggered two somatic APs and a large Ca^{2+} transient in stimulated dendritic segments (Fig. 3*g*,*h*). The tonic $GABA_A$ conductance reduced the AUC of ΔV_m induced by EPSP burst by approximately half, bringing it below the threshold for AP generation (Table 2; Fig. 3*g*). Consequently, the Ca^{2+} transient was proportionally reduced (Table 2; Fig. 3*f*, *h*). Further blockade of NMDARs had a small effect on the AUC but completely abolished the Ca^{2+} transient (Table 2, GABA + APV; Fig. 3*f*–*h*). NMDAR blockade without a tonic $GABA_A$ conductance abolished one of the two APs and thereby reduced the AUC (Table 2; Fig. 4*d*). This blockade also largely suppressed the Ca^{2+} transient (Table 2; Fig. 4*e*,*f*). Thus, the model of CA1 pyramidal neuron proposed by Poirazi et al. (2003) suggests that tonic $GABA_A$ conductances should have a more profound effect on the ΔV_m and Ca^{2+} transient induced by EPSP burst than on those induced by bAP/EPSP pairing.

Tonic $GABA_A$ conductance differentially affects responses to bAP/uEPSP pairing and uEPSP burst in CA1 pyramidal neuron

To confirm the model's prediction, we performed two-photon Ca^{2+} imaging in dendritic spines (Fig. 5*a*). The dendritic Ca^{2+} transients (ΔG/R) induced by bAPs alone were not significantly affected by GABA and subsequent 100 μM picrotoxin ($GABA_A$ antagonist) application (GABA: 100.2 ± 8.2% of control, $n = 9$, $p = 0.98$, one-sample *t*-test; picrotoxin: 96.0 ± 8.3% of control, $n = 9$, one-sample *t*-test). This finding suggests that the tonic $GABA_A$ conductance did not affect bAPs in imaged dendrites. This, however, does not rule out its action on more distal dendritic branches. bAP/EPSP pairing was mimicked by uEPSP, followed in 20 ms by the injection of depolarizing current through the patch pipette (Fig. 5*b*). EPSP burst was mimicked by repeated glutamate uncaging (4 times at 100 Hz) at four synapses and further referred to as uEPSP burst (Fig. 5*c*). The application of GABA had a small effect on the somatic ΔV_m induced by bAP/uEPSP pairing that was not statistically significant (ΔV_m AUC: 94 ± 2% of control, $n = 7$, $p = 0.07$, one-sample *t*-test; Fig. 5*d*,*e*). Indeed, ΔV_m induced by the bAP/uEPSP pairing was dominated by somatic AP that was insensitive to tonic $GABA_A$ conductances. Nevertheless, the Ca^{2+} transient induced by the bAP/uEPSP pairing was significantly reduced (peak ΔG/R: 86 ± 4% of control, $n = 6$, $p = 0.01$, one-sample *t*-test; Fig. 5*d*,*f*).

In agreement with the model's prediction, GABA reduced the number of APs induced by the uEPSP burst from 2 ± 0 to 1.1 ± 0.3 ($n = 6$, $p = 0.031$, paired-sample *t*-test, Fig. 5*d*); and as such, both the ΔV_m and the Ca^{2+} transient were significantly decreased (ΔV_m AUC: 76 ± 6% of control, $n = 6$, $p = 0.007$, one-sample *t*-test; ΔG/R: 71 ± 3% of control, $n = 6$, $p < 0.001$, one-sample *t*-test; Fig. 5*d*–*f*). Consistent with our hypothesis, this decrease was significantly larger than the decrease observed with the bAP/uEPSP pairing (ΔV_m AUC: $p = 0.013$, ΔG/R: $p = 0.014$, two-sample *t*-test; Fig. 5*d*–*f*)

The subsequent blockade of NMDARs with APV did not further decrease the ΔV_m in either case (ΔV_m AUC in GABA + APV: 95 ± 3% of control, $n = 7$ for bAP/uEPSP pairing; 76 ± 5% of control, n = 6 for uEPSP burst; Fig. 5*d*,*e*). However, the Ca^{2+} transients were further reduced to a similar level in both cases (ΔG/R in GABA + APV: 43 ± 4% of control, $n = 6$ for bAP/uEPSP pairing; 41 ± 4% of control, $n = 6$ for uEPSP burst; $p = 0.77$, two-sample *t*-test for difference between stimulations; Fig. 5*d*, *f*). These results demonstrate that the Ca^{2+} transients induced both by bAP/uEPSP pairing and by uEPSP burst in dendritic spines are partially mediated by NMDARs and are sensitive to tonic $GABA_A$ conductance. However, it is not clear to what extent tonic $GABA_A$ conductances affect the NMDAR-dependent and NMDAR-independent components of Ca^{2+} transients. To address this issue, we reversed the order of drug application: first, we applied APV and then GABA. APV had a small, non statistically significant, effect on the ΔV_m to bAP/uEPSP pairing (ΔV_m AUC: 94 ± 4% of control, $n = 7$; $p = 0.14$, one-sample *t*-test) but significantly reduced the ΔV_m to uEPSP burst (ΔV_m AUC: 76 ± 7% of control, $n = 8$; $p = 0.008$, one-sample *t*-test; $p = 0.03$, two-sample *t*-test for difference between stimulations; Fig. 6). Nevertheless, NMDAR blockade reduced Ca^{2+} transients in both cases by approximately half (ΔG/R: 46 ± 4% of control, $n = 6$ for bAP/uEPSP pairing; 53 ± 6% of control, $n = 6$ for uEPSP burst; $p = 0.285$, two-sample *t*-test for difference between stimulations; Fig. 6). Subsequent GABA application had a small effect on the ΔV_m (ΔV_m AUC: 84 ± 4% of control, $n = 6$ for bAP/uEPSP pairing; 73 ± 4% of control, $n = 6$ for uEPSP burst; $p = 0.086$, two-sample *t*-test for difference between stimulations; Fig. 6*b*) and Ca^{2+} transients in both cases (to 39 ± 4%, $n = 6$, for bAP/uEPSP pairing and 38 ± 3%, $n = 6$, for uEPSP burst; $p = 0.865$, two-sample *t*-test for difference between stimulations; Fig. 6*c*). Notably, NMDAR-independent Ca^{2+} transients were equal for both types of stimulation before and after the application of GABA. This finding suggests that the effect of tonic $GABA_A$ conductance on different forms of LTP is due to its action on NMDAR-mediated Ca^{2+} transients.

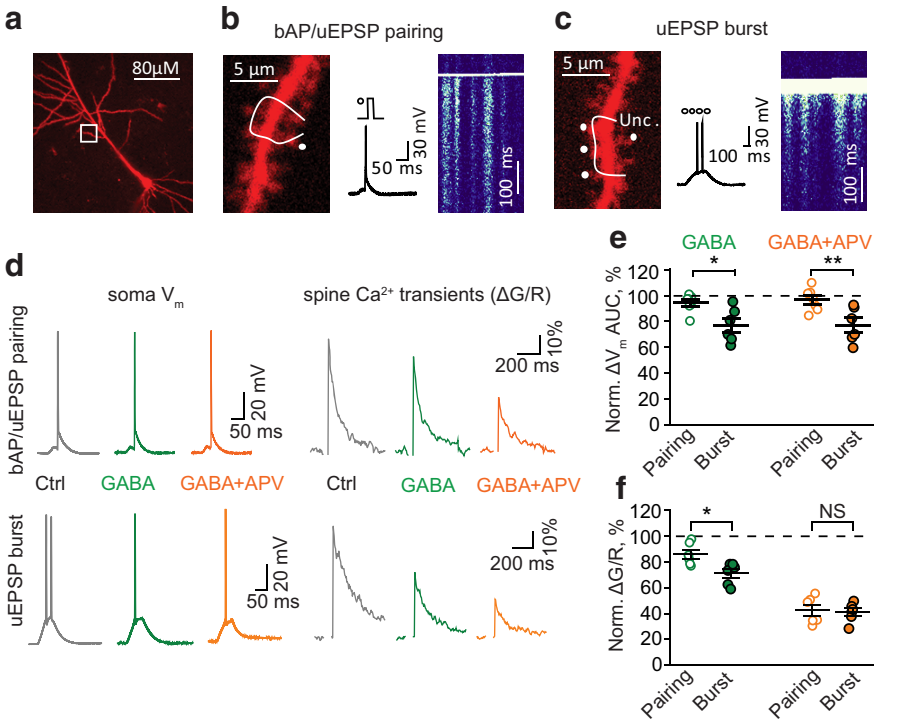

Figure 5. Tonic $GABA_A$ conductances differentially affect responses to bAP/uEPSP pairing and uEPSP burst in CA1 pyramidal neurons. ***a***, Representative image of a CA1 pyramidal neuron filled with the morphologic tracer AlexaFluor-594 (50 μM). White box represents a second-order dendritic branch used for Ca^{2+} imaging. ***b***, Left, Zoomed-in dendritic branch with a line-scan trajectory (white line) and an uncaging spot (Unc., white dot). Middle, The bAP/uEPSP pairing protocol (uncaging dot and current injection step) and corresponding V_m change in the soma. Right, A line-scan image in the Fluo-4F channel showing Ca^{2+} transients in dendritic spines and the shaft crossed by the line scan. ***c***, Left, Zoomed-in dendritic branch with a line-scan trajectory (white line) and four uncaging spots (Unc., white dots). Middle, The uEPSP burst protocol (four uncaging episodes at 100 Hz) and corresponding V_m change in the soma. Right, A line-scan image in the Fluo-5F channel showing Ca^{2+} transients in dendritic spines and the shaft crossed by the line scan. ***d***, The ΔV_m in the soma (left column) and the Ca^{2+} transients in dendritic spines (ΔG/R, right column) triggered by bAP/uEPSP pairing (top row) and uEPSP burst (bottom row). Gray represents Control (Ctrl). Green represents GABA application. Orange represents Subsequent APV application. ***e***, The summary of data on the effect of GABA (green) and subsequent APV application (orange) on the AUC of the ΔV_m to bAP/uEPSP pairing (empty symbols) and uEPSP burst (filled symbols). ***f***, The summary of data on the effect of GABA (green) and subsequent APV application (orange) on the Ca^{2+} transients induced by bAP/uEPSP pairing (empty symbols) and uEPSP bursts (filled symbols). Data are mean ± SEM. NS, Not significant ($p > 0.05$). *$p < 0.05$; **$p < 0.01$; two-sample *t*-test.

Discussion

We show that tonic $GABA_A$ conductance suppresses tbLTP, but not stLTP. Both forms of plasticity require NMDARs, but these NMDARs are recruited by different mechanisms. At baseline, NMDARs are blocked by Mg^{2+} (Nowak et al., 1984). Depolarization of the postsynaptic neuron removes this block and enables ion movement through glutamate-bound NMDARs (Wu et al., 2012). While synaptic activity serves as a source of glutamate in both forms of plasticity, the manner in which the Mg^{2+} block is removed differs. In the case of tbLTP, the EPSP burst propagates to the soma and triggers APs, which propagate back and sum with the burst. The resulting depolarization unblocks NMDARs. Tonic $GABA_A$ conductances suppress the EPSP burst by shunting. The diminished EPSP burst is unable to trigger APs and recruits fewer NMDARs. Thus, tbLTP is reduced. In the case of stLTP, the Mg^{2+} block of NMDARs is removed by bAPs. The AP is a regenerative event mediated by significantly larger conductances than those of tonic $GABA_A$ or the underlying EPSP (Hausser et al., 2001). Indeed, we did not detect any significant effect of tonic $GABA_A$ conductances on AP parameters (threshold, amplitude, half-width) recorded in the soma. However, this finding does not reflect the effect of tonic $GABA_A$ conductances on bAPs in the dendrite. Dendrites have a lower density of Na^+ and K^+ channels than the axonal trigger zone, which determines the shape of the somatic AP (Lorincz and Nusser, 2010; Kole and Stuart, 2012; Kirizs et al., 2014). Nevertheless, the bAP-induced Ca^{2+} transients recorded

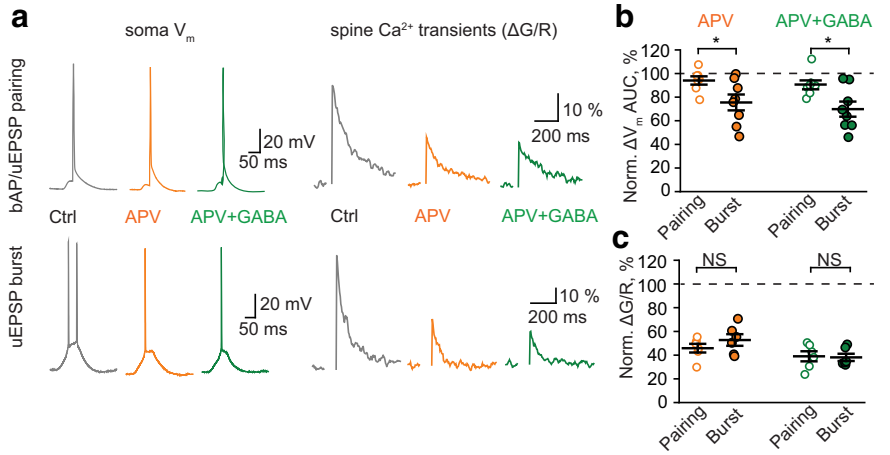

Figure 6. Tonic $GABA_A$ conductances have small effects on NMDAR-independent responses to bAP/uEPSP pairing and uEPSP burst in CA1 pyramidal neurons. ***a***, The $ΔV_m$ in the soma (left column) and the Ca^{2+} transients in dendritic spines (ΔG/R, right column) triggered by bAP/uEPSP pairing (top row) and uEPSP burst (bottom row). Gray represents Control (Ctrl). Orange represents APV application. Green represents Subsequent GABA application. ***b***, The summary of data on the effect of APV (orange) and subsequent GABA application (green) on the AUC of $ΔV_m$ to bAP/uEPSP pairing (empty symbols) and uEPSP burst (filled symbols). ***c***, The summary of data on the effect of APV (orange) and subsequent GABA application (green) on the Ca^{2+} transients induced by bAP/uEPSP pairing (empty symbols) and uEPSP burst (filled symbols). Data are mean ± SEM. NS, Not significant ($p > 0.05$). *$p < 0.05$, two-sample *t*-test.

with two-photon imaging were not significantly affected by GABA application. As a result, Ca^{2+} entry through NMDARs during bAP/EPSP pairing was decreased by tonic $GABA_A$ conductance significantly less than during EPSP burst. Consequently, no significant decrease in stLTP magnitude was detected, in contrast to tbLTP. We also demonstrated that the NMDAR-independent component of Ca^{2+} transients was similarly affected by GABA in the bAP/uEPSP pairing and uEPSP burst, suggesting that the observed effect is mediated by a GABA-dependent decrease of NMDAR-dependent Ca^{2+} transients during uEPSP burst stimulation.tbLTP can be linked to cell firing during theta rhythms, which is important for the encoding and retrieval of space- and time-related information (Hyman et al., 2003; Hasselmo and Stern, 2014; Larson and Munkacsy, 2015). stLTP can occur when the neuron receives synaptic inputs from many presynaptic cells and needs to choose which inputs are more relevant (Markram et al., 2012). Although the relevance of stLTP as a general model for synaptic plasticity is sometimes put into question (Lisman and Spruston, 2005, 2010), this phenomenon has been demonstrated in different species and brain regions *in vitro* and *in vivo* (Sjöström et al., 2008; Shulz and Jacob, 2010; Feldman, 2012; Gambino and Holtmaat, 2012; Jones et al., 2017). stLTP also has a broad appeal in computational neuroscience (Abbott and Nelson, 2000; Senn et al., 2001; Graupner and Brunel, 2007; Clopath et al., 2010; Vignoud et al., 2018). Our findings that stLTP is more resistant to tonic $GABA_A$ conductances than tbLTP may provide further insight into how the activity-dependent accumulation of ambient GABA can affect brain computations, learning, and memory. These findings can also be considered in the context of physiological/pathologic processes that control the magnitude of tonic $GABA_A$ conductance: densities and properties of extrasynaptic $GABA_A$ receptors, GABA release and clearance.

Tonic $GABA_A$ conductance is mediated by multiple and plastic $GABA_A$ receptors (Scimemi et al., 2005). The α5-subunit-containing $GABA_A$ receptor is a receptor subtype that contributes to the tonic inhibition of CA1 pyramidal neurons (Caraiscos et al., 2004). Notably, the pharmacological blockade of α5$GABA_A$ receptors enhances LTP in the CA1 region of the ventral hippocampus (Pofantis and Papatheodoropoulos, 2014). This receptor subtype also raises the LTP induction threshold in the dorsal hippocampus through predominantly nonsynaptic mechanisms and regulates certain forms of memory *in vivo* (Martin et al., 2010).

The change in tonic conductance magnitude due to modifications to receptor composition/density has been reported during development and in pathologic conditions (Brickley and Mody, 2012). Indeed, both increased tonic conductance and attenuated LTP were reported in animal models of epilepsy (Scimemi et al., 2005; Plata et al., 2018). In Alzheimer's disease, elevated concentrations of extracellular GABA occur due to GABA production and release by astrocytes (Wu et al., 2014), and the increased tonic $GABA_A$ conductance suppresses LTP in the hippocampal dentate gyrus in this disease.

Our results suggest that stLTP is insensitive to tonic $GABA_A$ conductance. However, it does not rule out that this form of plasticity remains under the control of other forms of GABAergic inhibition: for example, feedforward or feedback IPSPs curtailing EPSPs. The pairing of a single EPSP with a single AP, which we used in this study, is efficient in juvenile but not young adult mice or rats (Meredith et al., 2003). However, stLTP can still occur in response to EPSP pairing with a postsynaptic burst of APs. The blockade of $GABA_A$ receptors restores the ability of a single AP–EPSP pairing to induce LTP in adult rats. Therefore, this effect may be attributed to the maturation of the GABAergic system.

The transient emergence of $\alpha 4\beta\delta$ $GABA_A$ receptors on the spines of CA1 pyramidal neurons reduces activation of NMDARs and prevents tbLTP at puberty in mice (Shen et al., 2010). This effect of perisynaptic inhibition is more profound than the reduction of tbLTP mediated by tonic conductance reported in this study. Our work was conducted on prepubertal animals, where tonic conductance is mediated by $GABA_A$ receptors located on the dendritic shaft and soma. How the activation of perisynaptic $\alpha 4\beta\delta$ $GABA_A$ receptors would affect stLTP in puberty requires further investigation, although we speculate that stLTP may also be affected at puberty. Although spines are relatively electrically isolated and are weakly affected by dendritic conductance, the positioning of $GABA_A$ receptors on their surface may be a game-changer.

Ambient GABA concentrations build up due to GABA spillover and, thus, reflect neuronal activity (Glykys and Mody, 2007b; Song et al., 2013). Neuronal activity can also lead to an increase in extracellular GABA through astrocytes (Heja et al., 2012; Unichenko et al., 2013; Kirischuk et al., 2016). Synaptically released glutamate is taken up by astrocytic transporters along

with Na^+ in a 1:3 ratio. Intracellular Na^+ accumulation then reverses Na^+-dependent GABA transporters, which start to move GABA to the extracellular space.

A high level of neuronal activity is also required for tbLTP induction (Larson and Munkacsy, 2015). In many synapses, induction of LTP can lead to excessive excitability of the brain, seizures, and excitotoxicity. However, an accompanying increase in extracellular GABA reduces both the excitability and magnitude of tbLTP. Thus, the activity-dependent elevation of ambient GABA can serve as a protective mechanism to maintain balanced levels of brain excitation. This phenomenon is reminiscent of the homeostatic downregulation of individual cell excitability by the upregulation of *h*-channels following LTP induction (Fan et al., 2005; Wu et al., 2012). On the other hand, stLTP does not require a high rate of presynaptic firing but depends on the temporally correlated occurrence of synaptic inputs and postsynaptic APs. Thus, the induction of stLTP does not have to be associated with significant activity-dependent accumulation of extracellular GABA. Indeed, tonic $GABA_A$ conductance can be beneficial for stLTP, as stLTP is sensitive to spike jitter (Cui et al., 2018). Tonic $GABA_A$ conductance can reduce spike jitter by decreasing the membrane time constant (Wlodarczyk et al., 2013). In addition, we addressed only postsynaptic mechanisms by which tonic $GABA_A$ conductance can have a differential effect on LTP. In our model and glutamate uncaging experiments, we assumed synaptic release probability of 1, which means that each presynaptic AP triggers the vesicular release. Indeed, vesicular release probability in CA3-CA1 synapse varies from 0 to 1 (Hanse and Gustafsson, 2001). During burst stimulation, release probability can increase because of presynaptic facilitation and decrease because of depletion of immediately releasable vesicles. The activity-dependent facilitation occurs because of residual Ca^{2+} accumulation after each presynaptic AP and because of depolarization of presynaptic terminal by local elevation of extracellular K^+ (Shih et al., 2013). Most of the extracellular K^+ leaks to the synaptic cleft through postsynaptic NMDARs. When tonic $GABA_A$ conductance decreases activation of NMDARs, it also decreases NMDAR-mediated K^+ efflux and, hence, presynaptic facilitation. Reduced presynaptic facilitation will further decrease postsynaptic Ca^{2+} transients during burst stimulation and contribute to a more profound reduction of tbLTP.

In conclusion, brain states and activity that increase the tonic $GABA_A$ conductance suppress rate coding (tbLTP) but not temporal coding (stLTP) in the hippocampus. This phenomenon may have important implications for overall brain computations, learning, and memory.

References

Abbott LF, Nelson SB (2000) Synaptic plasticity: taming the beast. Nat Neurosci 3 Suppl:1178–1183.

Ade KK, Janssen MJ, Ortinski PI, Vicini S (2008) Differential tonic GABA conductances in striatal medium spiny neurons. J Neurosci 28:1185–1197.

Banke TG, McBain CJ (2006) GABAergic input onto CA3 hippocampal interneurons remains shunting throughout development. J Neurosci 26:11720–11725.

Ben-Ari Y (2002) Excitatory actions of GABA during development: the nature of the nurture. Nat Rev Neurosci 3:728–739.

Bereshpolova Y, Amitai Y, Gusev AG, Stoelzel CR, Swadlow HA (2007) Dendritic backpropagation and the state of the awake neocortex. J Neurosci 27:9392–9399.

Bracci E, Panzeri S (2006) Excitatory GABAergic effects in striatal projection neurons. J Neurophysiol 95:1285–1290.

Brickley SG, Mody I (2012) Extrasynaptic GABA(A) receptors: their function in the CNS and implications for disease. Neuron 73:23–34.

Brickley SG, Cull-Candy SG, Farrant M (1996) Development of a tonic form of synaptic inhibition in rat cerebellar granule cells resulting from persistent activation of GABAA receptors. J Physiol 497:753–759.

Brunner J, Szabadics J (2016) Analogue modulation of back-propagating action potentials enables dendritic hybrid signalling. Nat Commun 7:13033.

Caraiscos VB, Elliott EM, You-Ten KE, Cheng VY, Belelli D, Newell JG, Jackson MF, Lambert JJ, Rosahl TW, Wafford KA, MacDonald JF, Orser BA (2004) Tonic inhibition in mouse hippocampal CA1 pyramidal neurons is mediated by α5 subunit-containing γ-aminobutyric acid type A receptors. Proc Natl Acad Sci USA 101:3662–3667.

Chiang PH, Wu PY, Kuo TW, Liu YC, Chan CF, Chien TC, Cheng JK, Huang YY, Chiu CD, Lien CC (2012) GABA is depolarizing in hippocampal dentate granule cells of the adolescent and adult rats. J Neurosci 32:62–67.

Choi HJ, Lee CJ, Schroeder A, Kim YS, Jung SH, Kim JS, Kim do Y, Son EJ, Han HC, Hong SK, Colwell CS, Kim YI (2008) Excitatory actions of GABA in the suprachiasmatic nucleus. J Neurosci 28:5450–5459.

Clements J, Lester R, Tong G, Jahr C, Westbrook G (1992) The time course of glutamate in the synaptic cleft. Science 258:1498–1501.

Clopath C, Büsing L, Vasilaki E, Gerstner W (2010) Connectivity reflects coding: a model of voltage-based STDP with homeostasis. Nat Neurosci 13:344–352.

Cui Y, Prokin I, Mendes A, Berry H, Venance L (2018) Robustness of STDP to spike timing jitter. Sci Rep 8:8139.

Davies M (2003) The role of GABAA receptors in mediating the effects of alcohol in the central nervous system. J Psychiatry Neurosci 28:263–274.

Fan Y, Fricker D, Brager DH, Chen X, Lu HC, Chitwood RA, Johnston D (2005) Activity-dependent decrease of excitability in rat hippocampal neurons through increases in I(h). Nat Neurosci 8:1542–1551.

Farrant M, Nusser Z (2005) Variations on an inhibitory theme: phasic and tonic activation of GABA(A) receptors. Nat Rev Neurosci 6:215–229.

Feldman DE (2012) The spike-timing dependence of plasticity. Neuron 75:556–571.

Gambino F, Holtmaat A (2012) Spike-timing-dependent potentiation of sensory surround in the somatosensory cortex is facilitated by deprivation-mediated disinhibition. Neuron 75:490–502.

Gavrilov N, Golyagina I, Brazhe A, Scimemi A, Turlapov V, Semyanov A (2018) Astrocytic coverage of dendritic spines, dendritic shafts, and axonal boutons in hippocampal neuropil. Front Cell Neurosci 12:248.

Glykys J, Mody I (2007a) Activation of GABAA receptors: views from outside the synaptic cleft. Neuron 56:763–770.

Glykys J, Mody I (2007b) The main source of ambient GABA responsible for tonic inhibition in the mouse hippocampus. J Physiol 582:1163–1178.

Golding NL, Kath WL, Spruston N (2001) Dichotomy of action-potential backpropagation in CA1 pyramidal neuron dendrites. J Neurophysiol 86:2998–3010.

Graupner M, Brunel N (2007) STDP in a bistable synapse model based on CaMKII and associated signaling pathways. PLoS Comput Biol 3:e221.

Groen MR, Paulsen O, Pérez-Garci E, Nevian T, Wortel J, Dekker MP, Mansvelder HD, van Ooyen A, Meredith RM (2014) Development of dendritic tonic GABAergic inhibition regulates excitability and plasticity in CA1 pyramidal neurons. J Neurophysiol 112:287–299.

Haam J, Popescu IR, Morton LA, Halmos KC, Teruyama R, Ueta Y, Tasker JG (2012) GABA is excitatory in adult vasopressinergic neuroendocrine cells. J Neurosci 32:572–582.

Hanchar HJ, Dodson PD, Olsen RW, Otis TS, Wallner M (2005) Alcohol-induced motor impairment caused by increased extrasynaptic GABAA receptor activity. Nat Neurosci 8:339–345.

Hanse E, Gustafsson B (2001) Paired-pulse plasticity at the single release site level: an experimental and computational study. J Neurosci 21:8362–8369.

Hasselmo ME, Stern CE (2014) Theta rhythm and the encoding and retrieval of space and time. Neuroimage 85:656–666.

Hausser M, Major G, Stuart GJ (2001) Differential shunting of EPSPs by action potentials. Science 291:138–141.

Heja L, Nyitrai G, Kekesi O, Dobolyi A, Szabo P, Fiath R, Ulbert I, Pal-Szenthe B, Palkovits M, Kardos J (2012) Astrocytes convert network excitation to tonic inhibition of neurons. BMC Biol 10:26.

Herd MB, Belelli D, Lambert JJ (2007) Neurosteroid modulation of synaptic and extrasynaptic GABA(A) receptors. Pharmacol Ther 116:20–34.

Hines ML, Carnevale NT (1997) The NEURON simulation environment. Neural Comput 9:1179–1209.

Hyman JM, Wyble BP, Goyal V, Rossi CA, Hasselmo ME (2003) Stimulation in hippocampal region CA1 in behaving rats yields long-term potentiation when delivered to the peak of theta and long-term depression when delivered to the trough. J Neurosci 23:11725–11731.

Jack JJ, Redman SJ (1971) An electrical description of the motoneurone, and its application to the analysis of synaptic potentials. J Physiol 215:321–352.

Jones SL, To MS, Stuart GJ (2017) Dendritic small conductance calcium-activated potassium channels activated by action potentials suppress EPSPs and gate spike-timing dependent synaptic plasticity. eLife 6:e30333.

Kampa BM, Clements J, Jonas P, Stuart GJ (2004) Kinetics of Mg^{2+} unblock of NMDA receptors: implications for spike-timing dependent synaptic plasticity. J Physiol 556:337–345.

Kirischuk S, Héja L, Kardos J, Billups B (2016) Astrocyte sodium signaling and the regulation of neurotransmission. Glia 64:1655–1666.

Kirizs T, Kerti-Szigeti K, Lorincz A, Nusser Z (2014) Distinct axo-somato-dendritic distributions of three potassium channels in CA1 hippocampal pyramidal cells. Eur J Neurosci 39:1771–1783.

Kole MH, Stuart GJ (2012) Signal processing in the axon initial segment. Neuron 73:235–247.

Larson J, Munkacsy E (2015) Theta-burst LTP. Brain Res 1621:38–50.

Lisman J, Spruston N (2005) Postsynaptic depolarization requirements for LTP and LTD: a critique of spike timing-dependent plasticity. Nat Neurosci 8:839–841.

Lisman J, Spruston N (2010) Questions about STDP as a general model of synaptic plasticity. Front Synaptic Neurosci 2:140.

Lorincz A, Nusser Z (2010) Molecular identity of dendritic voltage-gated sodium channels. Science 328:906–909.

MacKenzie G, Maguire J (2013) Neurosteroids and GABAergic signaling in health and disease. Biomol Concepts 4:29–42.

Maguire J, Mody I (2007) Neurosteroid synthesis-mediated regulation of GABA(A) receptors: relevance to the ovarian cycle and stress. J Neurosci 27:2155–2162.

Maguire J, Mody I (2008) GABA(A)R plasticity during pregnancy: relevance to postpartum depression. Neuron 59:207–213.

Mann EO, Mody I (2010) Control of hippocampal gamma oscillation frequency by tonic inhibition and excitation of interneurons. Nat Neurosci 13:205–212.

Markram H, Gerstner W, Sjostrom PJ (2012) Spike-timing-dependent plasticity: a comprehensive overview. Front Synaptic Neurosci 4:2.

Martin LJ, Zurek AA, MacDonald JF, Roder JC, Jackson MF, Orser BA (2010) α5 $GABA_A$ receptor activity sets the threshold for long-term potentiation and constrains hippocampus-dependent memory. J Neurosci 30:5269–5282.

McCool BA (2011) Ethanol modulation of synaptic plasticity. Neuropharmacology 61:1097–1108.

Meredith RM, Floyer-Lea AM, Paulsen O (2003) Maturation of long-term potentiation induction rules in rodent hippocampus: role of GABAergic inhibition. J Neurosci 23:11142–11146.

Mitchell SJ, Silver RA (2003) Shunting inhibition modulates neuronal gain during synaptic excitation. Neuron 38:433–445.

Nevian T, Sakmann B (2004) Single spine Ca^{2+} signals evoked by coincident EPSPs and backpropagating action potentials in spiny stellate cells of layer 4 in the juvenile rat somatosensory barrel cortex. J Neurosci 24:1689–1699.

Nowak L, Bregestovski P, Ascher P, Herbet A, Prochiantz A (1984) Magnesium gates glutamate-activated channels in mouse central neurones. Nature 307:462–465.

Otmakhova NA, Otmakhov N, Lisman JE (2002) Pathway-specific properties of AMPA and NMDA-mediated transmission in CA1 hippocampal pyramidal cells. J Neurosci 22:1199–1207.

Pavlov I, Savtchenko LP, Kullmann DM, Semyanov A, Walker MC (2009) Outwardly rectifying tonically active GABA(A) receptors in pyramidal cells modulate neuronal offset, not gain. J Neurosci 29:15341–15350.

Pavlov I, Savtchenko LP, Song I, Koo J, Pimashkin A, Rusakov DA, Semyanov A (2014) Tonic GABA(A) conductance bidirectionally controls interneuron firing pattern and synchronization in the CA3 hippocampal network. Proc Natl Acad Sci USA 111:504–509.

Plata A, Lebedeva A, Denisov P, Nosova O, Postnikova TY, Pimashkin A, Brazhe A, Zaitsev AV, Rusakov DA, Semyanov A (2018) Astrocytic atrophy following status epilepticus parallels reduced Ca^{2+} activity and impaired synaptic plasticity in the rat hippocampus. Front Mol Neurosci 11:215.

Pofantis H, Papatheodoropoulos C (2014) The α5 GABAA receptor modulates the induction of long-term potentiation at ventral but not dorsal CA1 hippocampal synapses. Synapse 68:394–401.

Poirazi P, Brannon T, Mel BW (2003) Arithmetic of subthreshold synaptic summation in a model CA1 pyramidal cell. Neuron 37:977–987.

Rall W (1969) Time constants and electrotonic length of membrane cylinders and neurons. Biophys J 9:1483–1508.

Ruiz A, Campanac E, Scott RS, Rusakov DA, Kullmann DM (2010) Presynaptic GABAA receptors enhance transmission and LTP induction at hippocampal mossy fiber synapses. Nat Neurosci 13:431–438.

Scimemi A, Semyanov A, Sperk G, Kullmann D, Walker M (2005) Multiple and plastic receptors mediate tonic GABA(A) receptor currents in the hippocampus. J Neurosci 25:10016–10024.

Semyanov A (2003) Cell type specificity of GABA(A) receptor mediated signaling in the hippocampus. Curr Drug Targets CNS Neurol Disord 2:240–247.

Semyanov A, Walker M, Kullmann D (2003) GABA uptake regulates cortical excitability via cell type-specific tonic inhibition. Nat Neurosci 6:484–490.

Semyanov A, Walker M, Kullmann D, Silver R (2004) Tonically active GABA (A) receptors: modulating gain and maintaining the tone. Trends Neurosci 27:262–269.

Senn W, Markram H, Tsodyks M (2001) An algorithm for modifying neurotransmitter release probability based on pre- and postsynaptic spike timing. Neural Comput 13:35–67.

Shen H, Sabaliauskas N, Sherpa A, Fenton AA, Stelzer A, Aoki C, Smith SS (2010) A critical role for alpha4betadelta GABAA receptors in shaping learning deficits at puberty in mice. Science 327:1515–1518.

Shen H, Gong QH, Aoki C, Yuan M, Ruderman Y, Dattilo M, Williams K, Smith SS (2007) Reversal of neurosteroid effects at alpha4beta2delta GABAA receptors triggers anxiety at puberty. Nat Neurosci 10:469–477.

Shih PY, Savtchenko LP, Kamasawa N, Dembitskaya Y, McHugh TJ, Rusakov DA, Shigemoto R, Semyanov A (2013) Retrograde synaptic signaling mediated by K^+ efflux through postsynaptic NMDA receptors. Cell Rep 5:941–951.

Shulz DE, Jacob V (2010) Spike-timing-dependent plasticity in the intact brain: counteracting spurious spike coincidences. Front Synaptic Neurosci 2:137.

Sjöström PJ, Rancz EA, Roth A, Häusser M (2008) Dendritic excitability and synaptic plasticity. Physiol Rev 88:769–840.

Song I, Savtchenko L, Semyanov A (2011) Tonic excitation or inhibition is set by GABA(A) conductance in hippocampal interneurons. Nat Commun 2:376.

Song I, Volynski K, Brenner T, Ushkaryov Y, Walker M, Semyanov A (2013) Different transporter systems regulate extracellular GABA from vesicular and non-vesicular sources. Front Cell Neurosci 7:23.

Stell BM, Brickley SG, Tang CY, Farrant M, Mody I (2003) Neuroactive steroids reduce neuronal excitability by selectively enhancing tonic inhibition mediated by delta subunit-containing GABAA receptors. Proc Natl Acad Sci USA 100:14439–14444.

Szemes M, Davies RL, Garden CL, Usowicz MM (2013) Weaker control of the electrical properties of cerebellar granule cells by tonically active GABAA receptors in the Ts65Dn mouse model of Down's syndrome. Mol Brain 6:33.

Unichenko P, Dvorzhak A, Kirischuk S (2013) Transporter-mediated replacement of extracellular glutamate for GABA in the developing murine neocortex. Eur J Neurosci 38:3580–3588.

Urban-Ciecko J, Kossut M, Mozrzymas JW (2010) Sensory learning differentially affects GABAergic tonic currents in excitatory neurons and fast spiking interneurons in layer 4 of mouse barrel cortex. J Neurophysiol 104:746–754.

Vardya I, Drasbek KR, Dosa Z, Jensen K (2008) Cell type-specific GABA A receptor-mediated tonic inhibition in mouse neocortex. J Neurophysiol 100:526–532.

Vignoud G, Venance L, Touboul JD (2018) Interplay of multiple pathways and activity-dependent rules in STDP. PLoS Comput Biol 14:e1006184.

Wei W, Faria LC, Mody I (2004) Low ethanol concentrations selectively augment the tonic inhibition mediated by delta subunit-containing GABAA receptors in hippocampal neurons. J Neurosci 24:8379–8382.

Whissell PD, Eng D, Lecker I, Martin LJ, Wang DS, Orser BA (2013) Acutely increasing deltaGABA(A) receptor activity impairs memory and inhibits synaptic plasticity in the hippocampus. Front Neural Circuits 7:146.

Wlodarczyk AI, Xu C, Song I, Doronin M, Wu YW, Walker MC, Semyanov A (2013) Tonic GABA(A) conductance decreases membrane time constant and increases EPSP-spike precision in hippocampal pyramidal neurons. Front Neural Circuits 7:205.

Woodruff AR, Monyer H, Sah P (2006) GABAergic excitation in the basolateral amygdala. J Neurosci 26:11881–11887.

Wu YW, Grebenyuk S, McHugh TJ, Rusakov DA, Semyanov A (2012) Backpropagating action potentials enable detection of extrasynaptic glutamate by NMDA receptors. Cell Rep 1:495–505.

Wu Z, Guo Z, Gearing M, Chen G (2014) Tonic inhibition in dentate gyrus impairs long-term potentiation and memory in an Alzheimer's disease model. Nat Commun 5:4159.

Xia Y, Zhao Y, Yang M, Zeng S, Shu Y (2014) Regulation of action potential waveforms by axonal GABAA receptors in cortical pyramidal neurons. PLoS One 9:e100968.